

Coking and decoking during methanation and methane decomposition on Ni-Cu supported catalysts*

Cokebildung und Entcoking während der Methanbildung und des Methanzerfalls auf Ni-Cu-Trägerkatalysatoren

M.T. Tavares**, I. Alstrup and C.A.A. Bernardo

The effect of the composition of silica supported Ni-Cu alloy catalysts on the process of coking and decoking during methane decomposition and during methanation was considered. The kinetics of methanation was studied and compared to those of carbon deposition and of strong adsorption of hydrogen. Initiation of the formation of filamentous carbon formation on mono-metallic surfaces may take place if the ratio of the partial pressures, $p_{\text{CO}}/p_{\text{H}_2}$, is larger than 2 ($T < 673 \text{ K}$) or 1 ($T > 673 \text{ K}$). Once the process starts, the chemical potential of the gas phase may be reduced to lower values without interruption of filament growth. Besides, it was concluded that the methanation reaction includes two steps: the dissociative adsorption of CO and the hydrogenation of the adsorbed species. It was possible to establish the mechanism through which Cu affects the activity of Ni. The effect of the composition of the alloy catalysts on the methane formation and on the simultaneous carbon deposition indicates that those reactions belong to group I and to group II, respectively, following Ponec's classification. It was possible to find the optimal Cu concentration that maximises methanation and minimises carbon deposition. The kinetics of methane decomposition was also considered and is well described by adapting a model developed by other authors for Fe catalysts.

Der Einfluß der Zusammensetzung von Ni-Cu-Legierungen auf SiO_2 -Trägerkatalysator auf den Coking- und Entcokingprozeß während des Methanzerfalls und der Methanbildung wurde untersucht. Die Kinetik der Methanbildung wurde untersucht und verglichen mit der Kohlenstoffabscheidung und der Stärke der Adsorption von Wasserstoff. Der Start der Bildung von fadenförmigem Kohlenstoff auf einheitlichen Metalloberflächen kann stattfinden, wenn das Verhältnis der Partialdrücke $p_{\text{CO}}/p_{\text{H}_2}$ größer ist als 2 ($T < 673 \text{ K}$) oder 1 ($T > 673 \text{ K}$). Sobald der Prozeß beginnt, kann das chemische Potential der Gasphase vermindert werden zu niedrigeren Werten, ohne daß das Fadenwachstum abgebrochen wird. Weiterhin wurde geschlußfolgert, daß die Methanbildungsreaktion zwei Schritte umfaßt: die dissoziative Adsorption von CO und die Hydrierung der adsorbierten Spezies. Es war möglich, den Mechanismus aufzustellen, durch den Cu die Aktivität von Nickel beeinflusst. Der Einfluß der Zusammensetzung der Legierungskatalysatoren auf die Methanbildung und die gleichzeitige Kohlenstoffabscheidung zeigt an, daß diese Reaktionen zu Gruppe I und zu Gruppe II gehören gemäß der Klassifizierung von Ponec. Es war möglich, die optimale Cu-Konzentration zu finden, die die maximale Methanbildung und minimale Kohlenstoffabscheidung bewirkt. Die Kinetik des Methanzerfalls wird auch betrachtet, diese wird gut beschrieben, in dem man ein Modell annimmt, das bereits von anderen Autoren für Eisenkatalysatoren entwickelt wurde.

1 Introduction

Methanation is an important process in the chemical industry for many purposes. It is one of the reaction steps in the

synthesis of Substitute of Natural Gas, SNG, a gaseous mixture rich in methane, particularly interesting in periods of oil crisis as it may be used as alternative fuel. The production of SNG includes several steps, but in general may be described by [1, 2]:



Several industrial processes lead to the SNG production [3, 4], but all of them are based on supported Ni catalysts.

Methanation also occurs during the Fischer-Tropsch process, the synthesis of hydrocarbons from CO and H_2 mixtures [5, 6]. The industrial production of ammonia is usually performed by means of an iron catalyst, which may be strongly poisoned by oxygen compounds. It is therefore important to remove CO and CO_2 from the synthesis gas. This is done by

* Presented at the EFC-workshop on 'Coking and Decoking', Porto, Portugal, 6/7 May 1999

** M.T. Tavares

Centro de Engenharia Biológica – IBQF,
Universidade do Minho,
P-4700 Braga (Portugal)

I. Alstrup

Haldor Topsøe Research Laboratories,
Nymøllevej 55, DK-2800 Lyngby (Denmark)

C.A.A. Bernardo

Departamento de Engenharia de Polímeros,
Universidade do Minho,
P-4800 Guimarães (Portugal)

methanation, performed by a nickel catalyst upstream the main reactor.

The raw material for many large scale industrial processes, such as ammonia and methanol synthesis is usually natural gas or oil, which is transformed into synthesis gas, i.e. a mixture of CO, CO₂ and H₂, by means of the steam reforming process performed on a nickel catalyst. In this process it is very important to control coking, which may not only cause deactivation of the catalyst by encapsulation, but may even result in destruction of the catalyst and blocking of the reactor because of excessive growth of filamentous carbon.

Carbon deposition occurs in all catalytic transformations of hydrocarbons and reactions like methanation and methane decomposition follow the general rule. The regeneration of those catalysts, when possible, may be performed by gasification with steam, oxygen, carbon dioxide or hydrogen. This operation may be quite expensive because of production interruption, and may promote catalyst sintering, as gasification reactions are very exothermic. So there is strong need of optimising the Ni catalysts properties so they may become more resistant to carbon deposition without significant loss of activity towards the desired reactions. Actually, the SPARG process developed by Haldor Topsøe, A/S, is based in partial poisoning of the Ni surface with sulphur [7]. In this case carbon formation is prevented by “ensemble control”. This can also be achieved by diluting the active metal with another one not active towards carbon deposition. This is an important reason for considering the behaviour of Ni-Cu alloys in the present work.

2 Filaments formation

Carbon deposits were classified by temperature programmed gasification as they may present different reactivities towards the gasification agent. In a study with Al₂O₃ supported Ni catalysts, where deposits were obtained from C₂H₄ and CO and afterwards gasified by H₂ and H₂O, with temperatures ranging from 550 K and 1273 K, different structures of carbon deposits were detected [8]: chemically adsorbed carbon, carbides, filamentous carbon of different structures, encapsulating carbon and graphite.

Lobo et al. [9] and Baker et al. [10] suggested, independently, that the filamentous carbon formation includes surface adsorption, followed by decomposition of the reagent, carbon diffusion through the metallic particle and precipitation in energetically favourable regions, ending with filament growth and particle detachment. Baker followed the process of carbon filament formation by Controlled Atmosphere Electron Microscopy (CAEM). It was suggested, then, that the temperature gradient between the gas-metal interface (where the exothermic decomposition of the reagent takes place) and the metal-filament interface (where the endothermic precipitation of the carbon in metal solution occurs) would be the driving force for carbon diffusion. This was strongly discussed, as filamentous carbon formation is also evident during endothermic reactions, like methane decomposition. Rostrup-Nielsen and Trimm [11] suggested that the driving force for carbon diffusion through the metallic particle is the concentration gradient established between the gas-metal and the metal-filament interfaces due to a difference in carbon activities.

Carbon accumulation on Fe catalysts and, later, on Ni catalysts, was considered by Manning and Reid [12] and these authors suggested the presence of an intermediate unstable

carbide that would decompose constantly into metal and carbon. In a comprehensive study on thermodynamics, mechanisms and filament morphology, Geus and co-workers [13–15] also suggested to invoke in the mechanism a constantly decomposing, metastable carbide controlling the thermodynamics of filamentous carbon formation. The driving force for carbon transportation through the metallic particle was supposed to be provided by a concentration gradient between different non-stoichiometric carbides.

This model could hardly explain the reversibility between the growth of filaments and the gasification of these deposits and, particularly, the fact that the transition between deposition and gasification, as well as the transition between the gasification and the deposition, occur at the same value of carbon activity of the gas phase. In fact, Figueiredo and co-workers [16, 17] studied the gasification of carbon filaments formed on Ni catalysts with hydrogen and steam by thermogravimetry and CAEM. The reversibility of filament growth was established and gasification was described by: i) dissociative adsorption of the reagent gas on the catalytic surface, ii) supply of carbon atoms from the deposit through the metallic particle or along its surface, iii) reaction between the adsorbed gas and carbon.

A comprehensive study presented by Alstrup [18] links kinetic data with surface science observations of the interaction between carbon atoms and distinct crystallographic surfaces of Ni. The model proposed incorporates an estimate by Tibbets [19] of the elastic energy of filaments, which explains the tubular form of the deposits. The deviation from graphite equilibrium is thus mainly accounted for by the elastic energy and the surface energy of the filaments. The interaction of methane with different crystallographic surfaces of Ni was studied by Auger electron spectroscopy and low energy electron diffraction and those observations allowed Alstrup to conclude that methane decomposition occurs on (110) and on (100) facets, as well as on surface kinks and edges. Atomic carbon rapidly migrates below the surface into the selvedge forming a surface carbide, functioning as a constant carbon source for diffusion through the particle. In the initiation period the particle is gradually being saturated by carbon. When saturation reaches (111) facets, it triggers a considerable crystallographic reconstruction of the particle. This reconstruction leads to faceting of the metallic particle and to its well known “pear shape”. The concentration gradient between surface carbide and metal-filament interface acts as a driving force for carbon diffusion through the particle. If the transport of heat, needed to maintain isothermal conditions, is limited, then carbon diffusion may be reduced by thermal gradient.

3 Bi-metallic surfaces

The establishment of the mechanism of a catalytic reaction requires characterisation of the solid phase under reaction conditions. Surface composition of Ni-Cu alloys does show some controversial aspects. In fact, surface enrichment in Cu was detected under certain conditions, as a function of temperature and past working circumstances. For small particles surface enrichment and bulk depletion of Cu led to the formulation of the “cherry model” [20]. In small particles the surface segregation driven by surface energy gain, is limited by mass balance. The surface segregation was studied by magnetic techniques, in-situ H₂ adsorption [21], by high resolution electron energy loss spectroscopy [22] and, in a more direct way, by Auger electron spectroscopy [23].

In spite the general acceptance of surface segregation of Cu in Ni-Cu alloys, *Dalmon* [24] concluded that the surface composition of his silica supported Ni-Cu catalysts particles was the same as the bulk composition. In the present studies clear evidence was obtained showing that the surface of the alloy particles of the silica supported Ni-Cu catalysts was enriched in Cu. However, interaction with the gas phase during reaction may change the surface composition. Also, even in vacuum the Cu segregation may not be valid for all bulk compositions. Some researchers have concluded from their experimental results that Ni segregate to the surface in Ni-Cu alloys with high concentration of Cu (> 84%), [25, 26]. When supported catalysts are reduced at high temperatures a strong metal-support interaction may be observed. Ni-Si alloys have been detected and they reduce the chemisorption capacity of Ni, as well as reaction activity.

Ni-Cu/SiO₂ pellets with a metallic catalytic area of 6.82 m² g⁻¹, determined by H₂ chemisorption, and with a B.E.T. area of 250 m² g⁻¹, determined by N₂ adsorption, were used in this study [27]. The pellets showed an average pore radius of 90 Å and no microporosity. Ni crystallites presented an average dimension of 250 Å. X-ray diffraction showed only one phase for alloys with higher concentration of nickel than copper. When concentration of copper was dominant two phases were detected, pure Cu and a Ni-Cu alloy.

4 Ensemble effects

The activity of a catalytic surface depends on the number of unoccupied neighbouring atoms of the catalytic metal needed for a reaction to occur. The larger the size of this group of neighbour atoms called "ensemble", the higher the sensibility of the reaction to surface dilution with an inactive element. If the ensemble size needed is only one surface atom, then activity depends linearly on the dilution of the active metal. Different dependencies on surface dilution of competing reactions may determine the selectivity of a catalytic reaction. Thus the selectivity may be optimised by ensemble control, i.e. by a pre-established surface dilution of the catalytic element. *Ponec* [28] reviewed the physical and catalytic properties of macroscopic Ni-Cu alloys and established that nominal compositions between 20% and 90% of Ni lead to surface compositions of 10% ± 6% Ni. Catalytic activity for those reactions which require only one Ni atom, should not be reduced more than one order of magnitude when Ni surface is diluted with Cu. Such reactions are classified as type I and include C-H, O-H and N-H breakage. Type II reactions, which include reactions where C-C, C-N and C-O bonds are broken, suffer a 15–20 fold rate reduction (or several orders of magnitude) with surface dilution. The latter reactions need several surface atoms or groups of atoms to proceed. They are sensitive to catalyst structure, the activity and selectivity depend on crystallite size and on structural properties of the catalyst.

The effect of surface dilution with copper on the different reactions, methanation and carbon deposition with and without H₂, is evident in Fig. 1. This graph also presents the amount of totally adsorbed H₂ and strongly adsorbed H₂ as functions of the bulk composition of the alloys. While the rate of methanation is reduced less than 75% with surface dilution, and even enhanced at small Cu concentrations (≤ 10% Cu), the carbon deposition rate in the presence of H₂ is reduced more than two orders of magnitude for Cu con-

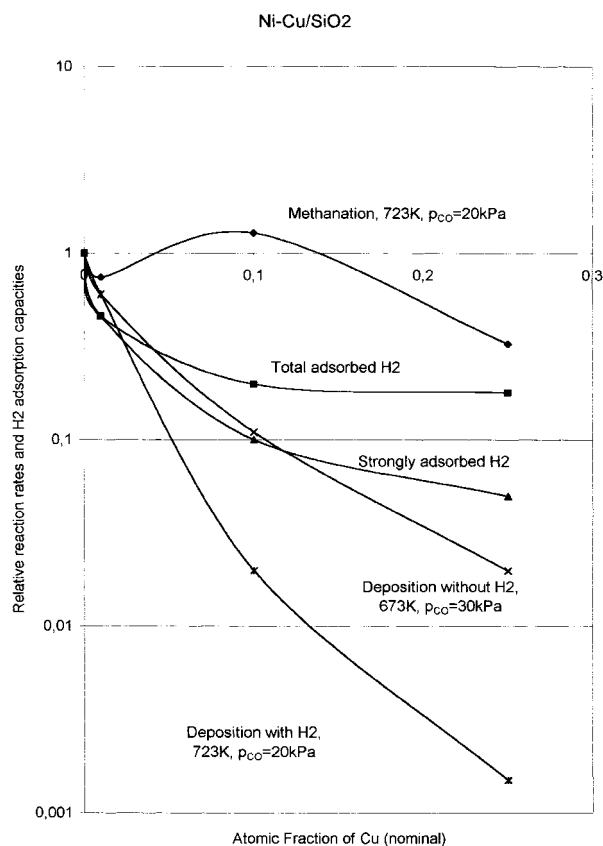


Fig. 1. Effect of surface dilution with Cu on rates of methanation, carbon deposition with and without hydrogen and on total and strong H₂ adsorption

Abb. 1. Einfluß der Oberflächenverdünnung mit Kupfer auf die Geschwindigkeiten der Methanbildung, der Kohlenstoffabscheidung mit und ohne Wasserstoff und auf die gesamte und starke Wasserstoffadsorption

centrations higher than 20%. Even for 10% Cu carbon deposition rate is reduced two orders of magnitude, while methanation rate increased. The effect of Cu is particularly evident for carbon deposition. In fact, the rate of this reaction is reduced much more than strongly adsorbed H₂. It requires more than the number of surface active sites needed for the chemisorption of gases and to catalyse type I reactions, indicating that this is a reaction type II, involving C-O links as foreseen by *Ponec* [28]. Methanation is not really affected by surface dilution and even a reaction rate enhancement was detected for 10% at Cu. This is a reaction type I, involving breaking of C-H bonds. The increase of the reaction rate was also foreseen by *Ponec*, justified by rate reduction of side reactions, more sensitive to surface dilution than the main reaction. Two factors may determine this process. The first one is the adsorption and the decomposition of CO, strongly affected by the dilution of the active metal. The other one is the adsorption of H₂ producing methane by reaction with the adsorbed species, gasifying the encapsulating carbon and preventing further adsorption. Carbon does not accumulate on the surface. It either disappears into the bulk or is hydrogenated and desorbs as methane.

Araki and *Ponec* studied methanation from CO and from CO₂, as well as CO decomposition and gasification of deposits formed on Ni and on Ni-Cu films, between 523 K and 623 K [29]. They also detected two reaction steps: carbon monoxide dissociation and gasification of the deposited car-

bon by the adsorbed hydrogen. As the dissociation of CO demands an ensemble of several atoms, methanation rate is strongly reduced by surface dilution of Ni with Cu.

The impact of Cu concentration on the formation rate of CH_4 , C_2H_6 and C_3H_8 , starting from CO and H_2 was described by *Dalmon* and *Martin* [30,31]:

$$r = r_{\text{Ni}} (1 - x)^N \quad (4)$$

where r_{Ni} is the reaction rate when the catalyst is pure Ni, x is the Cu fraction in the metallic phase and N is the number of unoccupied neighbouring Ni atoms needed in the active ensemble. *Dalmon* and *Martin* concluded that N is equal to 12 for methanation and to 20 for ethane and propane formation.

Data obtained in the present study indicates an ensemble of three atoms needed for methanation. The same size was defined for methane steam reforming, with the catalytic surface partially poisoned with sulphur [7]

5 Methanation on Ni and on Ni-Cu supported catalysts: kinetics

The methanation reaction was followed between 573 K and 748 K, catalysed by pure Ni and by its alloys [32, 33] and it was observed that carbon deposition process needs a minimum ratio between partial pressures of CO and of H_2 in order to start. Those studies indicated that $p_{\text{CO}}/p_{\text{H}_2} > 2$ allowed deposition to be detected. Once the process was started the pressure ratio could be reduced without interruption of deposition. This indicated that the initial nucleation is more demanding than steady-state growth. This effect was not observed for bi-metallic surfaces.

By adsorption-desorption studies different surface species were recognised and the global mechanism should include surface decomposition of carbon monoxide followed by successive hydrogenation of adsorbed species [34]. Carbon monoxide decomposition would be rate limiting at lower temperatures while gasification of the deposits would become slower at higher temperatures. Maximum rate was detected at 693 K.

6 Methane decomposition on Ni and on Ni-Cu supported catalysts: kinetics

Various kinetic models have been suggested for methane decomposition. In the simplest one it is assumed that the rate of filamentous carbon formation is proportional to carbon activity in the gas phase, independent of the nature of the carbon containing gas and applicable to endothermic as well as to exothermic reactions [35]. In fact, that proportionality was observed in thermodynamic conditions close to equilibrium and taking into account the difference of formation energy between graphite and filamentous carbon, which is $\Delta G = 7 \text{ kJ mol}^{-1}$ for an average crystallite size of 205 Å.

However, this linear relation was not observed for temperatures higher than 783 K. For these temperatures rate reduces with increasing chemical potential for deposition [36]. These observations could be explained by diffusional limitations and, in fact, they were detected by comparison between pellet and powder results, as may be seen in Fig. 2. Some simple calculations indicate a Knudsen regime as $D_{\text{K,eff}} = 2.725 \times 10^{-3} \text{ cm}^2 \text{ s}^{-1}$, while $D_{\text{CH}_4\text{-H}_2,\text{eff}} = 0.558 \text{ cm}^2 \text{ s}^{-1}$.

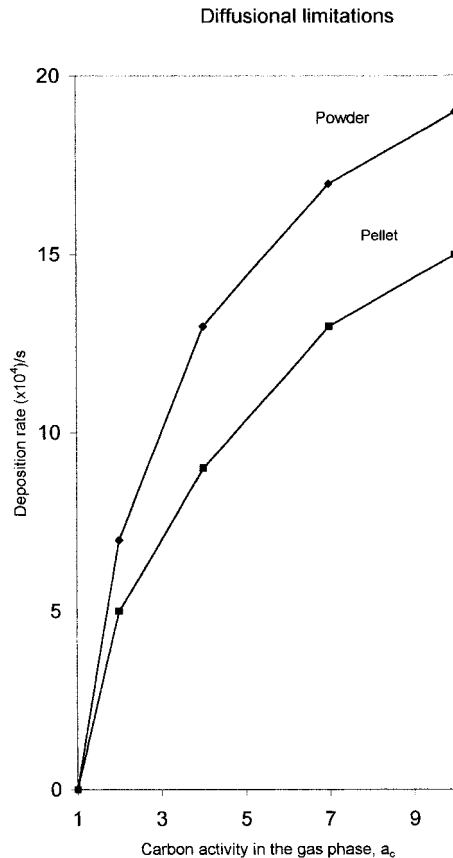


Fig. 2. Methane decomposition rates on a supported nickel catalyst as an extruded pellet and as a crushed powder

Abb. 2. Methanzerfallsgeschwindigkeiten auf einem Nickelträgerkatalysator in Form eines stranggepressten Pellets und als ein zerstoßenes Pulver

These values were obtained at 723 K and at 863 K they change to $D_{\text{K,eff}} = 2.977 \times 10^{-3} \text{ cm}^2 \text{ s}^{-1}$ and to $D_{\text{CH}_4\text{-H}_2,\text{eff}} = 0.795 \text{ cm}^2 \text{ s}^{-1}$. In addition to the observed mass transfer restrictions, deactivation of sites may contribute to the deviations to the proposed model at high temperatures.

Based on studies of carbon deposition on iron films *Grabke* [37] suggested a kinetic model for the dissociative adsorption of methane. In this model it is assumed that adsorbed methane is stepwise dehydrogenated. This model was adapted to supported Ni-Cu catalysts by assuming dissociative chemisorption of methane and by including subsurface migration of carbon, diffusion through the particle and precipitation into the carbon filament. It was concluded that the best mathematical fit to our experimental data was obtained when the dissociative adsorption of CH_4 or the dehydrogenation of adsorbed CH_3 is considered rate limiting [36, 38].

7 Conclusions

Filamentous carbon formation on monometallic catalysts during methanation starts only if the ratio between partial pressures of carbon monoxide and hydrogen is higher than 2 or than 1, depending on temperature. Once the process starts, carbon chemical potential in the gas phase may be reduced to lower values without interruption of the deposition process.

Methanation includes two reaction steps, the dissociative adsorption of CO and the hydrogenation of adsorbed species. The dependence of methanation rate and of simultaneous carbon deposition rate on the composition of the catalytic surface indicate that these reactions are type I and type II, respectively, according to Ponec's classification.

It was possible to find an optimal Cu concentration for Ni-Cu/SiO₂ catalysts that maximises CH₄ production and minimises carbon deposition. Among the catalysts considered that optimal composition was 10% at. Cu.

The experimental results on methane decomposition on those bi-metallic catalysts may be explained by a kinetic model developed by Grabke for the same reaction on iron films. The model includes dissociative adsorption of methane followed by stepwise dehydrogenation of the adsorbed species, equilibrium hydrogen surface coverage, dissolution and diffusion of adsorbed carbon. Good agreement between model and experimental rates is obtained when either the dissociative chemisorption of methane or the dehydrogenation of adsorbed CH₃ is rate limiting.

Diffusional transport restrictions are revealed during methane decomposition at high temperatures for catalysts with big amounts of accumulated carbon.

8 References

- [1] R. L. Ensell, H. J. F. Stroud: International Gas Research Conference, London, 1983.
- [2] K. R. Wild, A. Williams: 100th ATG Conference, Cannes, 1983.
- [3] H. S. Davies, J. A. Lacey, B. H. Thompson: 34th Autumn Research Meeting of the Institution of Gas Engineers, London, 1968.
- [4] J. A. Lacey: Institution of Gas Engineers, Scottish Section, 1985.
- [5] H. Wise, J. McCarty, J. Oudar: in: Deactivation and Poisoning of Catalysts, (Eds. J. Oudar and H. Wise), Dekker, 1985, pp. 1.
- [6] J. R. Rostrup-Nielsen: in: Progress in Catalyst Deactivation, (Ed. J. L. Figueiredo), Martinus Nijhoff, 1982, pp. 209.
- [7] J. R. Rostrup-Nielsen: J. Catal. 33 (1974) 184.
- [8] J. G. McCarty, P. Y. Hou, D. Sheridan, H. Wise: Am. Chem. Soc. Symp. Ser. 202 (1982) 253.
- [9] L. S. Lobo, D. L. Trimm, J. L. Figueiredo: in: Proceedings of the 5th International Congress on Catalysis, Florida, 1972, 2 (Ed. J. W. Hightower) Amsterdam (1973) 1125.
- [10] R. T. K. Baker, M. A. Barber, P. S. Harris, F. S. Feates, R. J. Waite: J. Catal. 26 (1972) 51.
- [11] J. R. Rostrup-Nielsen, D. L. Trimm: J. Catal. 48 (1977) 155.
- [12] M. P. Manning, R. C. Reid: Ind. Eng. Chem. Process Des. Dev. 16 (1977) 358.
- [13] P. K. de Bokx, A. J. H. M. Kock, E. Boellaard, W. Klop, J. W. Geus: J. Catal. 96 (1985) 454.
- [14] A. J. H. M. Kock, P. K. de Bokx, E. Boellaard, W. Klop, J. W. Geus: J. Catal. 96 (1985) 468.
- [15] E. Boellaard, P. K. de Bokx, A. J. H. M. Kock, J. W. Geus: J. Catal. 96 (1985) 481.
- [16] J. L. Figueiredo, C. A. Bernardo, J. J. Chludzinski, Jr., R. T. K. Baker: J. Catal. 110 (1988) 127.
- [17] J. L. Figueiredo, D. L. Trimm: J. Catal. 40 (1975) 154.
- [18] I. Alstrup: J. Catal. 109 (1988) 241.
- [19] G. G. Tibbets: J. Crystal Growth 66 (1984) 632.
- [20] W. M. H. Sachtler, R. A. Van Santen: Applic. of Surf. Sci. 3 (1979) 121.
- [21] T. S. Cale, J. T. Richardson: J. Catal. 79 (1983) 378.
- [22] M. Matsuyama, K. Ashida, O. Takayasu, T. Takeuchi: J. Catal. 102 (1986) 309.
- [23] F. J. Kuijers, V. Ponec: Surface Sci. 68 (1977) 294.
- [24] J. A. Dalmon: J. Catal. 60 (1979) 325.
- [25] T. Sakurai, T. Hashizume, A. Jimbo, A. Sakai, S. Hyodo: Phys. Rev. Lett. 55 (1985) 514.
- [26] Y. C. Cheng: Phys. Rev. B 34 (1986) 7400.
- [27] I. Alstrup, M. T. Tavares: J. Catal. 139 (1993) 513.
- [28] V. Ponec: Int. J. Quantum Chem. 12 Suppl. 2 (1977) 1
- [29] M. Araki, V. Ponec: J. Catal. 44 (1976) 439.
- [30] J. A. Dalmon, G. A. Martin: in: Proceedings of the 7th International Congress on Catalysis, Tokyo, 1980, (Eds. T. Seiyama, K. Tanabe), Elsevier, New York, (1981), pp. 402.
- [31] J. A. Dalmon, G. A. Martin: J. Catal. 84 (1983) 45.
- [32] D. C. Gardner, C. H. Bartholomew: Ind. Eng. Chem. Prod. Res. Dev. 20 (1981) 80.
- [33] D. C. Gardner, C. H. Bartholomew: Ind. Eng. Chem. Fundam. 20 (1981) 229.
- [34] M. T. Tavares, I. Alstrup, C. A. Bernardo, J. R. Rostrup-Nielsen: J. Catal. 158 (1996) 402.
- [35] M. Audier, M. Coulon: Carbon 23 (1985) 317.
- [36] I. Alstrup, M. T. Tavares: J. Catal. 135 (1992) 147.
- [37] H. J. Grabke: Metall. Trans. 1 (1970) 2972.
- [38] I. Alstrup, M. T. Tavares, C. A. Bernardo, O. Sørensen, J. R. Rostrup-Nielsen: Materials and Corrosion 49 (1998) 367.

(Received: August 5, 1999)

W 3388